

PAPER • OPEN ACCESS

## Multi-frequency ODMR of Nitrogen-Vacancy Color Centers in Diamond Crystals in zero magnetic fields

To cite this article: A K Dmitriev and A K Vershovskii 2018 *J. Phys.: Conf. Ser.* **1135** 012051

View the [article online](#) for updates and enhancements.



**IOP | ebooks™**

Bringing you innovative digital publishing with leading voices to create your essential collection of books in STEM research.

Start exploring the collection - download the first chapter of every title for free.

# Multi-frequency ODMR of Nitrogen-Vacancy Color Centers in Diamond Crystals in zero magnetic fields

A K Dmitriev and A K Vershovskii

Ioffe Institute, Russian Academy of Sciences, St. Petersburg, 194021 Russia

E-mail: alexdmk777@gmail.com, antver@mail.ioffe.ru

**Abstract.** Techniques of optical detection of magnetic resonance, as applied to the nitrogen-vacancy center in diamond, provide a tool for controlling both electron and nuclear spins. These techniques generally use a combination of microwave (MW) drive field for electronic spin transitions and radiofrequency (RF) drive field for nuclear spin transitions. They are most effective in strong magnetic fields where levels anticrossing (LAC) occurs; therefore NV spin system dynamics is mostly studied under these conditions. Nevertheless, zero-field LAC can probably also be used for controlling electron and nuclear spin states as well for exciting narrow resonances for metrological application, and these perspectives are not yet properly investigated. Here we present two-quantum resonances appearing in ODMR spectra of NV centers in bulk diamond under multi-frequency (MW+RF) resonance excitation in zero and ultra-low magnetic fields, and discuss their specifics.

## 1. Introduction

The methods based on optically detected magnetic resonance (ODMR), as applied to negatively charged nitrogen vacancy (NV) color centers in diamond crystals, has brought forth new methods of high-resolution quantum magnetometry [1-3], as well as new methods of controlling electron and nuclear spins. The latter are considered to be very suitable for quantum information processing because of their very long compared to other solid-state objects relaxation time [4,5]. Typically, combined microwave (MW) and radiofrequency (RF) excitation [6-11] or the electron spin-echo envelope modulation methods [12] are used to address a chosen spin state, allowing for various multi-quantum resonances most thoroughly studied in [11]. Various schemes of hole-burning using multi-frequency MW and RF excitation were discussed in [12,13]; methods of all-optical excitation ODMR at two frequencies separated by the ground-state zero-field splitting were proposed in [14]. The methods of spin control are most effective in strong magnetic fields (0.05 or 0.1 T) where levels anticrossing (LAC) [4,5,11,13] in excited or ground state occurs.

However, LAC also occurs in zero magnetic field [15], and perspectives of using it for controlling electron and nuclear spin states as well as for exciting narrow resonances for metrological application are to be studied yet.

Here we present results of investigations of ODMR spectra of NV centers in bulk diamond in zero magnetic fields using multi-frequency (MW+RF) resonance excitation and demonstrate multi-quantum resonances due to the zero-field levels crossing and anticrossing.



## 2. Energy structure of the ground-state of NV center

Level structure of  $^3A_2$  ground state in external magnetic field  $\vec{B}$  is defined by the Hamiltonian [16,17]:

$$H = D(S_z^2 - \frac{1}{3}\vec{S}^2) + E(S_x^2 - S_y^2) + g_s\mu_B\vec{B}\cdot\vec{S} + A_{\parallel}S_zI_z + A_{\perp}(S_xI_x + S_yI_y) + PI_z^2 - g_I\mu_N\vec{B}\cdot\vec{I}, \quad (1)$$

where  $\mu_B = h\cdot 13.996\cdot 10^9$  Hz/T is the Bohr magneton,  $\vec{I}$  is the  $^{14}\text{N}$  nuclear ( $I = 1$ ),  $\vec{S}$  is the electron spin of NV center ( $S = 1$ ),  $\mu_N = h\cdot 7.622\cdot 10^6$  Hz/T is the nuclear magneton,  $D = 2.87$  GHz and  $E$  are axial and transverse zero-field splitting (ZFS) parameters,  $g_s = 2.003$  and  $g_I = 0.403$  are electron and nuclear g-factors,  $A_{\parallel} = -2.16$  MHz and  $A_{\perp} = -2.7$  MHz are axial and transverse hyperfine splitting parameters,  $P = 4.95$  MHz is the quadrupole splitting parameter. Denote eigenstates of the ground state  $|m_S, m_I\rangle$ ; for the nitrogen isotope  $^{14}\text{N}$  both electronic and nuclear spin projections take values  $m_S, m_I = 0, \pm 1$ .

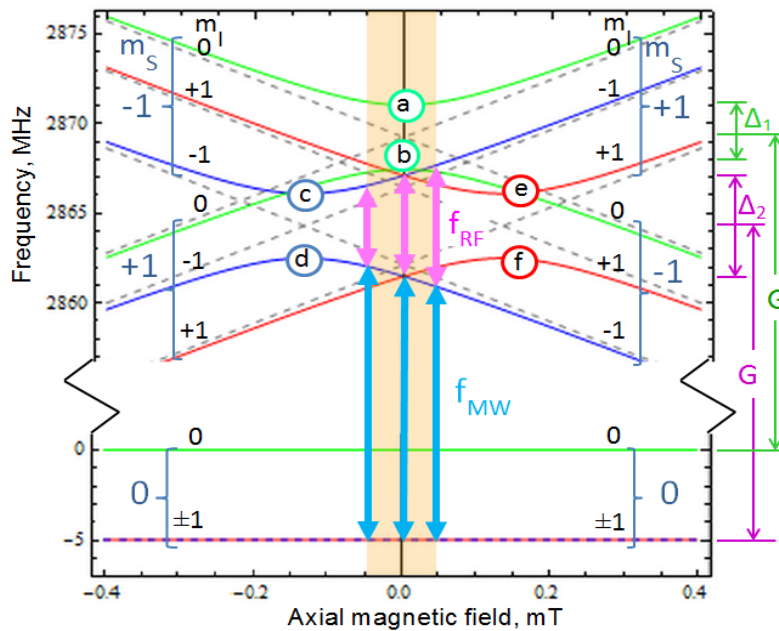


**Figure 1.** NV center ground-state splitting frequencies dependence on axial local magnetic field, calculated for a diamond crystal with transverse ZFS parameter  $E = 1.8$  MHz. Dashed lines represent pure quantum states, solid lines are mixed states denoted by circled letters. Arrows represent MW and RF drive fields. Colourfilled is a magnetic field range where two-quantum resonances can be observed.

Energy structure of NV center in zero and ultra-weak fields is more complex than in strong ones (Fig.1); it contains both levels crossings and anticrossings, partially masked by the crystal internal fields inhomogeneity. Each NV center in a bulk sample is affected by local magnetic field  $\vec{B}_L$ ; transverse component of this field together with strain field causes LAC. Therefore pure energy states  $|\pm 1, 0\rangle$  at  $B \approx 0$  mix in superpositions

$$\begin{aligned} |a\rangle &= a^- \cdot |-1, 0\rangle + a^+ \cdot |+1, 0\rangle \\ |b\rangle &= b^- \cdot |+1, 0\rangle + b^+ \cdot |-1, 0\rangle \end{aligned} \quad (2)$$

and pure energy states  $|\pm 1, \pm 1\rangle$  mix in superpositions

$$\begin{aligned} |c\rangle &= c^- \cdot |-1, -1\rangle + c^+ \cdot |+1, -1\rangle \\ |d\rangle &= d^- \cdot |+1, -1\rangle + d^+ \cdot |-1, -1\rangle \\ |e\rangle &= e^- \cdot |-1, +1\rangle + e^+ \cdot |+1, +1\rangle \end{aligned} \quad (3)$$

$$|f\rangle = f \cdot |+I, +I\rangle + f^* \cdot |-I, +I\rangle$$

The dependency of energy levels and corresponding frequencies on magnetic field  $B$  in low fields is substantially nonlinear. This structure was investigated in details in [15].

### 3. Experimental

The experimental setup was described in [18]: a synthetic diamond of SDB1085 60/70 grade (manufactured by Element Six) with dimensions  $0.1 \times 0.3 \times 0.3$  mm was subjected to electron irradiation ( $5 \cdot 10^{18}$  cm $^{-2}$ ) and subsequent annealing in Ar at 800°C for 2 hours. The crystal was used at a room temperature; it was fixed with an optically transparent glue to the end of an optical fiber with a core diameter of 0.9 mm; the wide fiber aperture ensured effective collection of the PL signal at the cost of losing  $\sim 90\%$  of pumping light. The pumping and detection efficiencies were further increased by covering the outer surfaces of the diamond and the end of the optical fiber with a non-conductive reflective coating.

The pumping beam (15 mW at a wavelength of 532 nm) was focused on the second end of the fiber, and the PL signal was collected from the same end. Given an overall pumping efficiency of less than 10%, the pumping power was far below the optimum [9]. We used low-frequency amplitude modulation of in order to subtract the fluorescence background.

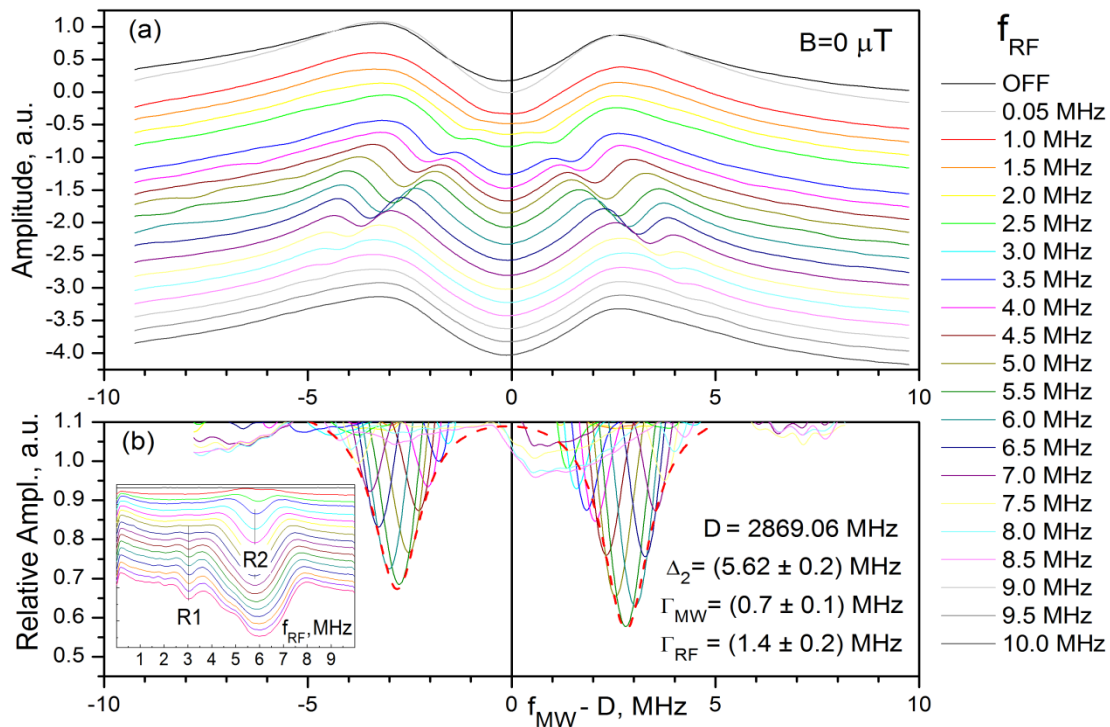


**Figure 2.** **a** ODMR spectra recorded at zero external field at different radiofrequencies  $f_{RF}$ ; upper curve is normal ODMR signal, two symmetrical hollows are two-quantum resonances (R2) arising when conditions (3) are fulfilled. **b** an envelope of R2 resonances; amplitudes are normalized to ones obtained under single-frequency MW excitation. Inset: ODMR dependence on RF frequency at linearly increasing from top to bottom RF drive field intensities.

We excited multi-frequency ODMR in  $B = (0 \div 0.15)$  mT using MW drive field  $f_{MW}$  in combination with additional RF field  $f_{RF}$ . This way we have recorded a narrow (approximately 0.25 MHz HWHM in respect to MW drive field) resonance, here in after referred to as R1 (see inset in Fig.2), arising under conditions

$$\begin{aligned} f_{RF} &\approx \Delta_1, \\ f_{MW} &\approx D, \end{aligned} \quad (4)$$

where  $\Delta_1 = (3.0 \pm 0.2)$  MHz. Unexpectedly, we also have found a wider (about 0.5 MHz HWHM at minimal RF field intensity) and stronger resonance R2 (Fig.2a) appearing at much lower RF intensities under conditions

$$\begin{aligned} f_{RF} &\approx \Delta_2, \\ f_{MW} \pm \frac{1}{2}f_{RF} &= D, \end{aligned} \quad (5)$$

where  $\Delta_2 = (5.62 \pm 0.2)$  MHz. The linewidth of the resonance envelope (Fig.2b) with respect to MW and RF drive fields was found to be  $\Gamma_{MW}/2\pi = (0.7 \pm 0.1)$  MHz and  $\Gamma_{RF}/2\pi = (1.4 \pm 0.2)$  MHz correspondingly. The frequencies of both resonances proved to be insensitive to  $B$ , as well as their relative amplitudes (normalized to ones obtained under single-frequency MW excitation).

#### 4. Discussion

Our calculations show that, for given diamond sample, frequency value  $\Delta_1$  corresponds to the splitting between states  $|a\rangle$  and  $|b\rangle$  at local axial field  $B_L = 0$  (see Fig.1), and  $\Delta_2$  corresponds to the splitting between states  $|c\rangle$ ,  $|e\rangle$  and  $|d\rangle$ ,  $|f\rangle$  at  $B_L = 0$ . As it follows from Fig.1, equations (4) and (5) describe two different two-quantum resonances:

Equation (4): transitions  $|0, 0\rangle \leftrightarrow |b\rangle \leftrightarrow |a\rangle$  (resonance R1);

Equation (5): transitions  $|0, -1\rangle \leftrightarrow |d\rangle \leftrightarrow |c\rangle$  and  $|0, +1\rangle \leftrightarrow |f\rangle \leftrightarrow |e\rangle$  (resonance R2).

There are also mirror reflections of both resonances in high-frequency wing of MW spectra (Fig.2), corresponding to the two-quantum transitions  $|0, 0\rangle \leftrightarrow |a\rangle \leftrightarrow |b\rangle$ , etc. Note that "two-quantum" here not necessary refers to the simultaneous absorption of MW and RF photons. This process may also consist of two stages: 1) since optical pumping mostly populates level  $m_S = 0$  [3], MW drive field transfers the excess of population to the states  $|b\rangle$ ,  $|d\rangle$ ,  $|f\rangle$  (or  $|a\rangle$ ,  $|c\rangle$ ,  $|e\rangle$ , depending on the sign of its frequency detuning, and 2) the RF field induces transitions  $|b\rangle \leftrightarrow |a\rangle$ ,  $|d\rangle \leftrightarrow |c\rangle$ ,  $|f\rangle \leftrightarrow |e\rangle$ , thus equalizing population of the states involved.

To explain how these resonances can be observed in a wide frequency range at  $B = 0$  one must take into consideration the inhomogeneity of the local axial magnetic field  $B_L$ : the width of its distribution usually is of order of tenths of microtesla. Therefore two-quantum resonance conditions (4), (5) require different frequency combinations for different NV centers depending on their local field values. The effect due to the inhomogeneity of strain electric field causing local shifts of transverse ZFS parameter is similar to the effect due to the inhomogeneity of  $B_L$ .

Variety of similar multi-frequency resonances arising due to excited state LAC in strong (51 mT) field was studied in [11]. Still, the resonances R1 and R2 discovered in zero field in the frame of this work show some peculiarities:

*First*, resonances due to the two-quantum transition described above should be of the same sign as normal ODMR signal obtained under single-frequency MW excitation, but both R1 and R2 are of opposite sign.

*Second*, RF-driven transitions between states with  $|Am_S + Am_I| > 1$  are forbidden since they can not be induced by single RF photon carrying unit moment; therefore schemes proposed above are not feasible outside LAC, which partially cancels this forbiddance. Note that equation (5), when applied to the ground-state levels scheme (Fig.1), unambiguously indicates that the R2 resonance transition is driven by one MW and one RF photon.

*Third*, if we suppose that these transition occur due to LAC (which seems to be true for R1), their amplitudes should be maximal at LAC center – in case of R2, at  $B_L = B_{LAC} \approx \pm 0.15$  mT (points (c)–(f) at Fig.1). Nevertheless, the amplitude of R2 reaches its maximal value at  $f_{RF} = \Delta_2$ , i.e. at  $B_L = 0$ .

Knowing the linewidth of the resonance envelope  $\Gamma_{MW}$ , we can estimate the boundaries of the range where R2 can be observed:  $|B_L| < \Gamma_{MW}/(g_S \mu_B / \hbar) \approx 0.025$  mT, so  $|B_L| \ll |B_{LAC}|$ . Therefore we can state that this resonance is not only due to LAC described by (3). It is more likely that it appears at level

crossing of the states  $|c\rangle$  and  $|e\rangle$ , and/or  $|d\rangle$  and  $|f\rangle$ ; or, taking into consideration that, according to Fig.1, at  $B_L = 0$  we can to some extent neglect LAC effects, it may as well be zero-field level crossing of the states  $|\pm 1, \pm 1\rangle$ , allowing for electron-nuclear spin-flips.

As to the first two oddities listed above, they both can be explained if we suppose that RF field does not drive transitions between levels  $\Delta m_{S,I} = \pm 2$ , but removes these levels from interaction with MW drive field, as it happens in three-levels  $\Lambda$ -schemes due to coherent population trapping effect [19].

## 5. Conclusions

We report on detection two different two-quantum resonances in zero-field ODMR spectra of NV center in diamond induced by applying an additional RF field. These resonances can only be driven when the axial local magnetic field satisfies condition  $|B_L| < 0.025$  mT (in case of our diamond sample), and therefore we can assert that they are due to the zero-field levels crossing. We attribute both resonances to the certain levels of NV center zero-field structure, but the mechanisms of their MW and RF excitation are to be studied yet.

## References

- [1] Taylor J M, Cappellaro P, Childress L, Jiang L, Budker D, Hemmer P R, Yacoby A, Walsworth R and Lukin M D 2008 *Nat. Phys.* **4** 810
- [2] Balasubramanian G, Chan I Y, Kolesov R, Al-Hmoud M, Tisler J, Shin C, Kim C, Wojcik A, Hemmer P R, Krueger A, Hanke T, Leitenstorfer A, Bratschitsch R, Jelezko F and Wrachtrup J 2008 *Nature* **455** 648
- [3] Acosta V M, Bauch E, Jarmola A, Zipp L J, Ledbetter M P and Budker D 2010 *Appl. Phys. Lett.* **97** 174104
- [4] Jelezko F, Gaebel T, Popa I, Domhan M, Gruber A and Wrachtrup J 2004 *Phys. Rev. Lett.* **93** 130501
- [5] Jacques V, Neumann P, Beck J, Markham M, Twitchen D, Meijer J, Kaiser F, Balasubramanian G, Jelezko F and Wrachtrup J 2009 *Phys. Rev. Lett.* **102** 057403
- [6] Gurudev Dutt M V, Childress L, Jiang L, Togan E, Maze J, Jelezko F, Zibrov A S, Hemmer P R and Lukin M D 2007 *Science* **316** 1312
- [7] Neumann P, Mizuochi N, Rempp F, Hemmer P, Watanabe H, Yamasaki S, Jacques V, Gaebel T, Jelezko F and Wrachtrup J 2008 *Science* **320** 1326
- [8] Jiang L, Hodges J S, Maze J R, Maurer P, Taylor J M, Cory D G, Hemmer P R, Walsworth R L, Yacoby A, Zibrov A S and Lukin M D 2009 *Science* **326** 267
- [9] Smeltzer B, McIntyre J and Childress L 2009 *Phys. Rev. A* **80** 050302
- [10] Steiner M, Neumann P, Beck J, Jelezko F and Wrachtrup J 2010 *Phys. Rev. B* **81** 035205
- [11] Childress L and McIntyre J 2010 *Phys. Rev. A* **82** 033839
- [12] Manson N B and Wei C 1994 *Journal of Luminescence* **58** 158
- [13] Kehayias P, Mrozek M, Acosta V M, Jarmola A, Rudnicki D S, Folman R, Gawlik W and Budker D 2014 *Phys. Rev. B* **89** 245202
- [14] Acosta V M, Jensen K, Santori C, Budker D and Beausoleil R G 2013 *Phys. Rev. Lett.* **110** 213605
- [15] Clevenson H, Chen E H, Dolde F, Teale C, Englund D and Braje D 2016 *Phys. Rev. A* **94** 021401
- [16] Felton S, Edmonds A M, Newton M E, Martineau P M, Fisher D, Twitchen D J and Baker J M 2009 *Phys. Rev. B* **79** 075203
- [17] Fischer R, Jarmola A, Kehayias P and Budker D 2013 *Phys. Rev. B* **87** 125207
- [18] Dmitriev A K and Vershovskii A K 2016 *JOSA B* **33** B1-B4
- [19] Arimondo E and Orriols G 1976 *Lett. Nuovo Cimento Soc. Ital. Fis.* **17** 333